2018 IEEE Conference on Decision and Control (CDC)
Miami Beach, FL, USA, Dec. 17-19, 2018

Dissipation of Emergent Traffic Waves in Stop-and-Go Traffic Using a Supervisory Controller

Rahul Kumar Bhadani, Benedetto Piccoli, Benjamin Seibold, Jonathan Sprinkle and Daniel Work

Abstract— **This paper presents the use of a quadratic band controller in an autonomous vehicle (AV) to regulate emergent traffic waves resulting from traffic congestion. The controller dampens the emergent traffic waves through modulating its velocity according to the relative distance and velocity of the immediately preceding vehicle in the flow. At the same time, it prevents any collision within the range specified by the design parameters. The approach is based on a configurable quadratic band that allows smooth transitions between (i) no modification to the desired velocity; (ii) braking to match the speed of the preceding vehicle; and (iii) braking to avoid collision with the lead vehicle. By assuming that the lead vehicle's velocity will be oscillatory, the controller's smooth transition between modes permits any vehicle following the AV to have a smoother reference velocity. The configurable quadratic band allows design parameters, such as actuator and computation delays as well as the dynamics of vehicle deceleration, to be taken into account when constructing the controller. Experimental data, software-in-the-loop distributed simulation, and results from physical platform performance in an experiment with 21 human-driven vehicles are presented. Analysis shows that the design parameters used in constructing the quadratic band controller are met, and assumptions regarding the oscillatory nature of emergent traffic waves are valid.**

I. Introduction

The growing number of vehicles, especially in urban areas, has resulted in operation near the saturation point of transportation infrastructure, giving rise to myriad problems such as traffic congestion, accidents, transportation delay and increased vehicle emissions [1]. The cost of congestion is estimated to be $124 billion per year in the USA [2]. Traffic congestion arises due to a number of factors including highway merges, faulty human decisions e.g. abrupt lane changing and increased vehicular density. However, previous research has shown that traffic waves due to congestion emerge even without infrastructure bottlenecks [3], [4]. As a part of ongoing effort towards smart cities [5], Autonomous Vehicles (AVs) are regarded as key elements of an approach that could alleviate problems such as these, through reduced need of ownership as well as intelligent control.

In addition to practical limitations of cost, the design of such intelligent controllers is constrained by (i) the rate at which sensor updates are available; (ii) the accuracy of those sensors; (iii) computation and communication delays; and (iv) actuator dynamics. Moreover, any controller implemented must satisfy the overarching design goal that a vehicle following the AV should be able to rely on the AVs behavior being predictable. Thus, fast-acting controllers or controllers whose strategy include subtle changes in velocity with the goal of reducing traffic waves may not be effective. That is, the controllers may not impact congestion if the follower vehicle drives more conservatively due to confusion over the (self-driving) lead vehicle's behavior.

With an expectation of increased participation of AVs on the roads—co-existent with human-driven vehicles—we are motivated to demonstrate the validity of the assumption that emergent traffic waves can be dampened through the actions of only a small number (e.g., 5%) of intelligent vehicles in the flow. These controllers were tested in simulation, and in hardware with a cadre of human drivers was shown to be effective in [6]. Although the results of the traffic experiment are known, the specific design and analysis of the controller in use has not been published elsewhere.

Contribution

This paper, being a continuation of [6], describes a controller that smoothly changes the velocity of the AV from its reference velocity (i.e., the velocity at which the flow dynamics of traffic are expected to be stable) to the velocity of the lead vehicle (i.e., the vehicle directly in front of the AV) if it is apparent that inaction may result in a need for braking to avoid collision. The result is called the *Followerstopper* controller, a controller that maintains a reference velocity in the flow (*follower*) but can avoid the need to execute collision avoidance style braking (*stopper*), since an underlying assumption of the flow dynamics is that the lead vehicle may be either speeding up, or slowing down, as the AV approaches. The key to the approach is to design the switching modes such that acceleration and deceleration do not result in wave propagation during congested traffic. The approach is described in detail in this paper, backed by driving characterization based on experimental data, software-in-the-loop simulation and phase-portrait analysis of the result that have not been discussed in [6].

Related works

We separate collision avoidance, where steering commands can be used to avoid obstacles in the path [7], [8], [9], from the scenario where velocity control is intended to avoid collision with another vehicle or object moving along the same path. It is relevant to consider that predictive

R. Bhadani is with Dept. of Electrical and Computer Engineering, The University of Arizona, Tucson, AZ 85721, USA. *rahulbhadani@email.arizona.edu*

J. Sprinkle is with Dept. of Electrical and Computer Engineering, The University of Arizona, Tucson, AZ 85721, USA. *sprinkjm@email.arizona.edu*

B. Seibold is with Dept. of Mathematics, Temple University, Philadelphia, PA 19122, USA. *seibold@temple.edu*

D. Work is with Dept. of Civil and Environmental Engineering, Vanderbilt University, Nashville, Tennessee 37240, USA. *dan.work@vanderbilt.edu*

B. Piccoli is with Dept. of Applied Mathematics, Rutgers University, Camden, NJ 08901, USA. *piccoli@camden.rutgers.edu*

978-1-5386-1395-5/18/$31.00 ©2018 IEEE

controllers which take into account the state of the AV and its environment are intended to ensure that collision doesn't occur. Controllers that depend on high-bandwidth trusted communication between vehicles permit close platooning [10], [11] but violate our assumption that human-driven vehicles make up a large portion of the vehicles in the flow. There are several approaches for collision-avoidance techniques in the context of autonomous driving. In [12], the authors use model predictive control where an assumption of vehicular network or vehicle-to-infrastructure network has been made. In spite of these development, research in collision avoidance has not been jointly considered with a goal of smooth transition between different velocity profiles to prevent unsafe scenario in stop-and-go traffic. Previous works require sophisticated and expensive sensors and pose significant challenges in terms of algorithmic and software integration [13], [14], [15]. The underlying assumption they make is the presence of inter-vehicle communication which may not be available in those case where an AV encounters human-driven vehicles. Moreover, none of these works provide any approach which dissipates phantom traffic jams to create uniform flow of traffic.

II. Formulation

Consider the i^{th} vehicle in the flow (see Figure 1), which is following vehicle $i-1$ (referred to as the *lead vehicle* or *the lead*), and is followed by vehicle $i+1$ (the *following vehicle*). For this paper, we assume that the primary control input is reference longitudinal velocity for the AV. Thus we have a plant $\dot{v} = f(v,u)$ where the control input u is the desired vehicle velocity, and v is the output velocity of the vehicle. The plant function f is based on filtering of vehicle headway and smoothing of subsequent derivatives to deliver real-time results with acceptable accuracy to attain safe driving behavior [16]. The dynamics of f are abstracted as max. & min. accelerations, $\dot{v}_{max}, \dot{v}_{min}$ noting that $\dot{v}_{min} < 0$.

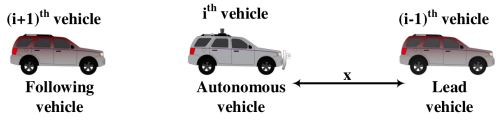

Fig. 1: leader-follower configuration

The distance between the front bumper of vehicle i and the rear bumper of the lead $i-1$ is defined as $\mathbf{x}_i^{i-1}$. For simplicity, we drop the super and subscripts and let the AV be the i^{th} vehicle in the flow: thus $\mathbf{x} := \mathbf{x}_i^{i-1}$. Likewise, we define the relative velocity as the rate of change of relative distance, $\dot{\mathbf{x}} = \frac{d\mathbf{x}}{dt}$. Sources of disturbance in the formulation include delay and noise. Chief among these: (i) actuator delays in $f(\cdot,\cdot)$; (ii) filter delays for calculation of $\mathbf{x}$, (iii) transport delays in implementing the updated control strategy due to computation rate of the controller. Regarding noise, we assume Gaussian error for velocity and distance.

Note: The distance estimate could vary significantly if a different feature set is tracked on the lead. Jumps in distance are handled algorithmically to avoid spurious velocity estimates based on naive distance estimates: this adds to the potential delay due to the larger time-window required for estimation that a different feature has been tracked. This problem has been addressed in [16] in the context of [6] and further in this paper.

Let r be a reference longitudinal velocity, which may (or may not) be generated by a function that takes into account vehicle following or collision avoidance.

Problem Statement

Let $u = g(r, \mathbf{x}, \dot{\mathbf{x}})$ be a controller that may modify the reference longitudinal velocity r to generate an improved longitudinal velocity u that is passed on to the plant f for the AV. Then design g such that:

i) robustness parameters e.g. delay, and min. separation distance may be provided as design parameters;
ii) dynamical parameters such as maximum deceleration may be used as design parameters; and
iii) the output velocity u changes smoothly from the reference velocity r to a velocity that potentially dampens (rather than amplify) disturbances in velocity.

With this design, ensure that:

a) collisions are avoided within maximum range and velocity estimates;
b) waves are dampened via smooth transitions; and
c) deceleration and acceleration profiles are representative of human drivers.

III. Approach

The controller takes a weighted sum approach to mixing signals based on a weighing function λ:

$$h = \lambda f_1 + (1-\lambda) f_2 \tag{1}$$

where f_1 and f_2 are two different signals, and $0 \leq \lambda \leq 1$ is used to smoothly weight how much of each signal should be used to produce the desired output signal h. Such an approach promises to map directly where we can consider the reference signal r as f_1, and the velocity of the lead as f_2. However, some modifications are required in order to enable design parameters such as min. separation distance, delay, etc. With aforementioned motivations in mind, the premise of the controller is to command the reference velocity r whenever safe. It commands a suitable lower velocity $u < r$ whenever safety is required based on the lead's velocity v_{lead} and the distance $\mathbf{x}$ between the front vehicle of the AV and the rear of the lead. The lead's velocity is obtained as $v_{i-1} = v_i + \dot{\mathbf{x}}$, where v_i is the velocity of the AV.

The reference velocity r is an input from an external controller to our supervisory controller with an output u. Using the gap $\mathbf{x}$ and relative velocity $\dot{\mathbf{x}}$, we define a phase space, divided into three regions: (i) a safe region, where $u = r$; (ii) a stopping region where zero velocity is commanded; (iii) adaptive region, where weighted average of desired velocity and lead's velocity is commanded. The adaptive region has two parts that we describe shortly. The boundaries between regions are parabolas in the $\mathbf{x}\dot{\mathbf{x}}$ phase

space (trajectories that the AV–lead pair would traverse when decelerating at constant rates), defined as

$$\mathbf{x}_j = \omega_j + \frac{1}{2\alpha_j}(\dot{\mathbf{x}}^*)^2 \text{ for j = 1, 2, 3.} \tag{2}$$

$\dot{\mathbf{x}}^* = min(\dot{\mathbf{x}}, 0)$ is the negative arm of velocity difference, i.e., the case of the AV falling behind is treated just like the case of $v_{AV} = v_{lead}$. The significance of parameters ω_j are discussed in Section IV. α_j are deceleration in m/s^2 which define the parabolic curve of the quadratic band. In practice deceleration values come from the characteristic of the driving behavior of vehicle in the stop-and-go traffic. It is discussed in detail in Section IV.

Thus, the commanded velocity is defined as:

$$u = \begin{cases} 0, & \text{if } \mathbf{x} \leq \mathbf{x}_1 \\ v\frac{\mathbf{x}-\mathbf{x}_1}{\mathbf{x}_2-\mathbf{x}_1}, & \text{if } \mathbf{x}_1 < \mathbf{x} \leq \mathbf{x}_2 \\ v+(r-v)\frac{\mathbf{x}-\mathbf{x}_2}{\mathbf{x}_3-\mathbf{x}_2}, & \text{if } \mathbf{x}_2 < \mathbf{x} \leq \mathbf{x}_3 \\ r, & \text{if } \mathbf{x}_3 < \mathbf{x} \end{cases}. \tag{3}$$

where,

$$v = \min(\max(v_{\text{lead}}, 0), r) \tag{4}$$

which is the lead's velocity (if positive) or the desired velocity, whichever is smaller.

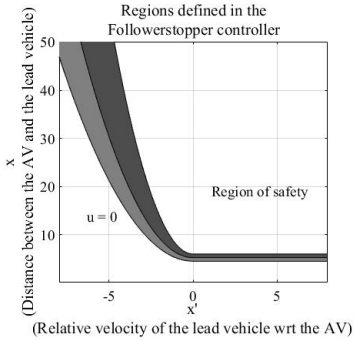

Fig. 2: Quadratic band showing the operating regions of the Followerstopper controller

Based on the quadratic band in the phase space plot, the controller output is velocity r whenever safe but a suitably lower velocity u whenever AV finds itself operating in the unsafe region. In the adaptive region ($\mathbf{x}_1 < \mathbf{x} \leq \mathbf{x}_3$), the commanded velocity changes smoothly from stopping (u = 0, for short headways) to safe driving ($u = r$, for large headways), via a transition involving the lead's velocity.

IV. Design

The design criteria explained in Section II require human-driving characterization of the vehicle involved in the controller-assisted driving. In our controller design, the effect of system delay is absorbed in the minimum permissible distance between the lead and the AV. Therefore, we designed a quadratic band on $\mathbf{x}\dot{\mathbf{x}}$ phase-space divided into two parts. The quadratic band enabled the controller to offer smoother transition between modes of the velocity profile.

We conducted some experiments with the leader-follower system on an open track to gather parameters of traffic

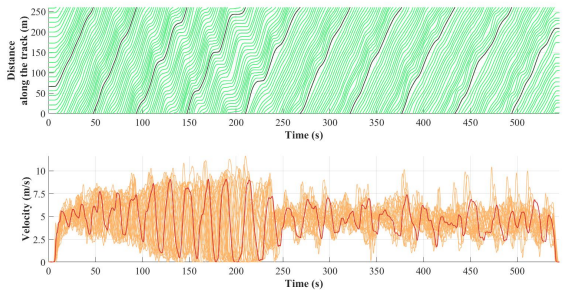

Fig. 3: Traffic waves produced during one of the experiments to characterize unassisted driving behavior. **Top:** The distance of each vehicle involved in the ring road experiment with respect to the time. Origin was chosen as an arbitrary point on the ring. **Bottom:** Velocity profiles of all vehicles involved in the experiment. The darker curve represents velocity profile of the CAT Vehicle, the AV used in our experiments. In this case all vehicles including the CAT Vehicle were driven manually.

dynamics without any sensor-assisted driving. In context with the work in [6], Sugiyama's experiment [3] was replicated with few modifications to suit US driving conventions. We determined the minimum permissible distance between two vehicles to be $4.5m$, the required value of parameter ω_1 in (2). This defines the $\mathbf{x}$ intercept in the linear region of lower quadratic curve as shown in Figure 2. To capture the system delay (e.g., time delay, delay due to computation, etc.) which may affect control performance, we expanded the quadratic curve to a quadratic band with linear region of upper quadratic curve defined by the $\mathbf{x}$ intercept ω_3 = 6.0m. In the region of this band, the velocity command is adaptive based on the instantaneous relative velocity of the AV and the distance between the AV and the lead.

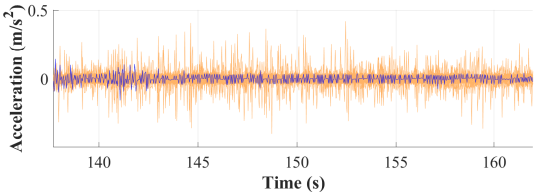

Fig. 4: Acceleration profile of vehicles involved in a ring-road experiment. The curve in the center is acceleration profile of the CAT Vehicle driven by a human without any controller assistance.

Our experiments provided some evidence about traffic bottlenecks and phantom jams in the form of an oscillatory nature of a vehicle's velocity in urban traffic as observed in Figure 3. From replication of Sugiyama's experiment, we inferred that almost all the time, the maximum value of acceleration/deceleration didn't exceed $0.5m/s^2$.

The acceleration profile of one of the replications is shown in Fig 4. We want the autonomous control to be representative of human driving, otherwise another human following an AV might behave erratically in response to unexpected braking or acceleration events by the preceding vehicle driving autonomously. Our objective is twofold: i) smooth transition from the reference velocity r to a velocity that potentially dampens the traffic waves, ii) maintaining a sufficient distance from the lead to prevent a collision.

Keeping these points in mind, we choose the deceleration value α_1 in (2) to be $0.5m/s^2$ for the AV to drive like

human with mild adjustments defined by the Followerstopper controller in (3). α_1 along with ω_1 stated above defines the parabolic portion of the curve in the phase space plot. We chose ω_3 to be $1.5m/s^2$ to define the upper curve of the quadratic band. α_3 along with ω_3 determines at what distance the adaptation of the velocity command for safety triggers and how fast or slow adaptation proceeds. We also split the band into two regions with an additional curve in the middle of the band defined by $\omega_2 = (\omega_1 + \omega_3)$ and $\alpha_2 = (\alpha_1 + \alpha_3)$. In this way, the quadratic band ensures a smooth transition when switching modes for maintaining a safe distance between vehicles and collision-avoidance. It is possible to split the quadratic band into more than two regions depending on the required behavior of the controller.

We validated our design with data obtained from one of the ring-road experiments that were used to characterize human driving behavior. Figure 5 demonstrates a scenario where the phase space curve goes well below $\mathbf{x} = 4.5m$ for several seconds, while in human control.

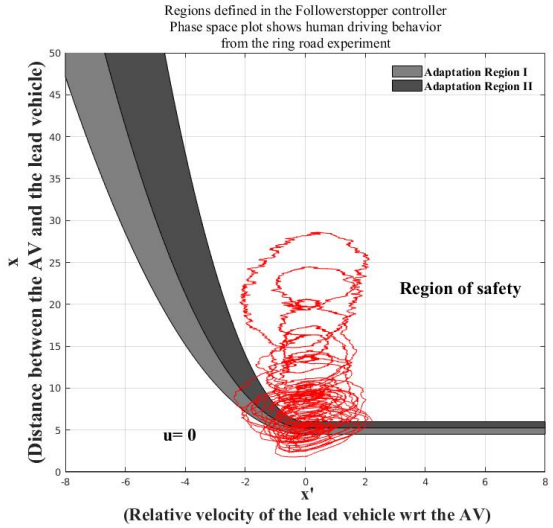

Fig. 5: $\mathbf{x}\dot{\mathbf{x}}$ Phase space plot for ring-road test 1 that was conducted to characterize human driving behavior. This phase space curve represents standard human driving behavior that is observed in an urban stop-and-go traffic. The phase space curve below $\mathbf{x} = 4.5m$ represents an undesirable state.

V. Implementation and Analysis

The controller defined in Section III uses The Robot Operating System (ROS) [17] and MATLAB for implementation. The CAT Vehicle used for autonomous driving in our experiment is based on ROS for high level control. The implementation of the Followerstopper uses the findings from open road experiments with a leader-follower system and ring-road experiments for an analysis of the controller and parameter tuning. Our implementation follows a series of steps that uses widely popular ROS packages and model-based design using Simulink. To begin with, we used formal modeling language provided by Simulink to design our controller. Initially we verified our design with synthetic data input and a model of the CAT Vehicle obtained from its system identification. The dynamics of the CAT Vehicle for our design verification uses a PID controller with K_p, K_i and K_d values being 44.6218, 72.7801, and 0.84327,with plant transfer function

$$T(s) = \frac{0.133}{s+0.5}. \tag{5}$$

The plant transfer function is a simplified first order model based on constant acceleration, valid in the regime of $0-8m/s$ with manually controlled steering (and autonomous velocity control). Results from one such simulation with reference velocity r and leader's velocity v_{lead} as sinusoidal inputs are shown in Fig 6. Our simulation result verified

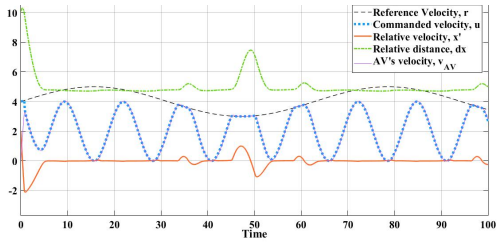

Fig. 6: Simulation of the Followerstopper with synthetic data. Reference velocity r and v_{lead} are provided with sinusoidal inputs. In this simulation the min distance between the lead and the AV was $4.7m$ with mean of $5.174m$ and std dev of 1.108.

that the controller design explained in Section IV met the constraints specified and minimum distance between the lead and the AV was less than ω_1 for most part. In the later part, we were able to utilize abstractions provided by Robotics System toolbox to interface with ROS. We replaced the synthetic data input and low level control dynamics in the simulink block mentioned in (5) with physics-based model of the AV implemented in Gazebo and ROS. The Robotics System Toolbox provides an executable specification of parameters that can be supplied at runtime. Following the design phase, we used the code generation feature of Simulink to generate C++ code which is a verified substitute for the model in the Software in the loop (SIL) simulation. We compared the results from design simulation with Simulink block with the results obtained from SIL simulation. In the next step, we used generated code to target the implementation in the CAT Vehicle. Results from SIL simulation demonstrated that we were able to prevent collision at the limit specified by our design parameter α_1 (see Fig 7).

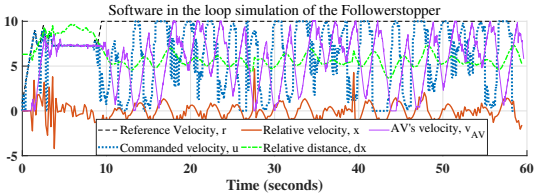

Fig. 7: SIL simulation of the Followerstopper with ROS and Gazebo and reference velocity $r = 10m/s$. Min. distance between the lead and the AV was 3.627m with median of 5.654m, mean 6.016m and std. dev. of 1.245m. The simulation used the real driving profile for the leader vehicle obtained from driving a car manually and injecting data into the simulation. Even though min distance is less than 4.5m, there are only 9 sample points less than 4.5m of $\mathbf{x}$ sparsely located in 60 seconds of simulation.

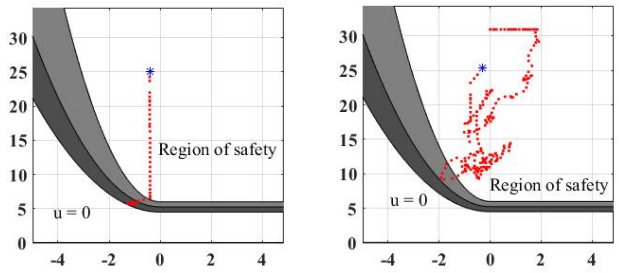

Fig. 8: $\mathbf{x}\dot{\mathbf{x}}$ phase space plot, the blue star denotes initial point of phase curve. Left: lead vehicle is at rest at some distance from the following vehicle. Once the controller is activated the following vehicle closes the gap upto a min. safe gap by controller-assisted driving. Right: the lead was given velocity input from joystick to drive like a human and the following vehicle drove with controller-assisted driving in safe manner.

Results from two different SIL simulation with ROS and Gazebo are shown: i) Figure 8a presents the reaction of the AV while approaching the lead that is stationary; ii) in Figure 8b velocity reference of the lead is given using a PS2 joystick, with the AV following autonomously with the assistance of the Followerstopper controller. In either case, the $\mathbf{x}\dot{\mathbf{x}}$ phase-space curve did not enter the undesired region of $u = 0$.

VI. Results

To test the wave-dampening effect of the Followerstopper, we recreated the Sugiyama experiment with one of the vehicles being driven autonomously using the Followerstopper. More details about this experiment can be found in [6]. The CAT Vehicle was initially under human control for first 126s into the experiment. We saw traffic waves at $t = 79s$. At $t = 126s$, we activated the Followerstopper controller and it was no longer under human control for velocity command. The trajectories of all the vehicles involved in the experiment with different reference velocity for entire duration is shown in Fig 9. When we look at the traffic wave between the time duration

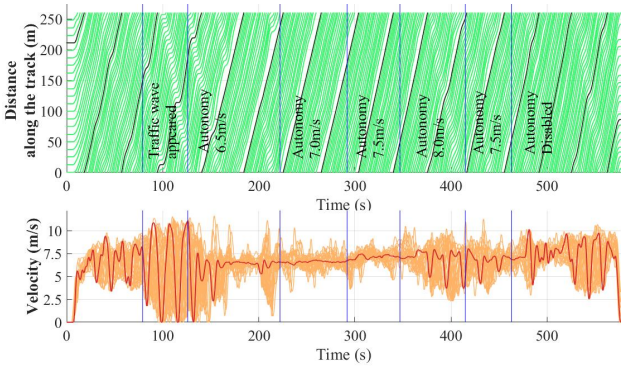

Fig. 9: Trajectories and velocity profiles of all the vehicles involved in the final experiment to test the wave-dampening effect of the Followerstopper controller.

of $t = 79 - 126s$, when the wave was dominant, we can easily observe the characteristic oscillatory nature of the velocity profile (lower half of Fig 9). During these 47s, all vehicles involved in the ring road experiment were constantly slowing down or speeding up, giving rise to stop-and-go traffic waves. The Followerstopper controller was activated at $t = 126s$ with a reference speed of $r = 6.5m/s$, which in practice may come from some other controller. Fig 9 as well as 10 show that while the oscillatory nature of the

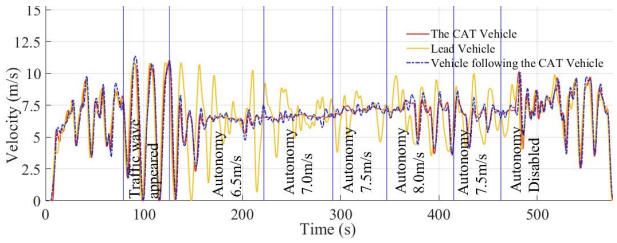

Fig. 10: Velocity profiles of the CAT Vehicle (i.e. AV) and its preceding vehicle with controller-assisted driving.

lead's velocity was still observable right after $t = 126s$ from the experiment, we saw a remarkable dissipation in the amplitude of oscillation as time elapsed. In Fig 11, a portion of the phase curve in red gradients denotes oscillatory behavior of the AV velocity profile during first few seconds after the controller was activated.

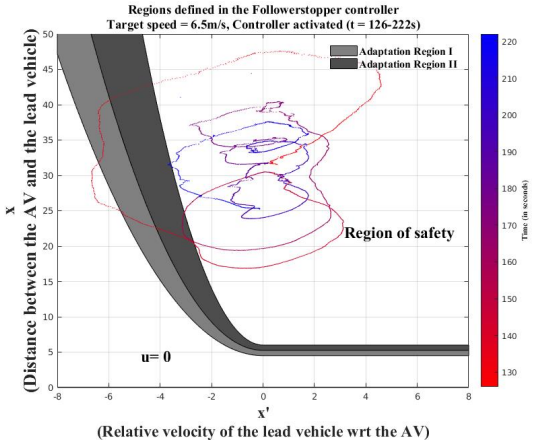

Fig. 11: Controller activated with $r = 6.5m/s$ at t = 126s. In the beginning of this autonomy mode, there are noticeable oscillations in the velocity profile of the AV, which dampens with time. Although the phase curve shown in unsafe region is due to the oscillatory nature of velocity profile in the beginning of this autonomy phase, the $\mathbf{x}\dot{\mathbf{x}}$ curve stays above $\mathbf{x} = 4.5m$. Design of Followerstopper ensures that the AV avoids passing through the state of potential collision by sending $u = 0$ command and eventually switching to the region of safety.

It can be understood by a significantly higher value of acceleration and deceleration as shown in Fig 12 at the beginning of autonomy phase with $r = 6.5m/s$. During this time, deceleration was greater than equal to $1m/s^2$. Nevertheless, the characteristic acceleration profile of human driving that we have discussed in Section IV is preserved. This ensures safety while following an AV. At $t = 222s$, we changed reference velocity r to be $7.0m/s$, which continued till $t = 292s$. We found the wave dissipation to be greatest during this period as shown in Fig 9. The phase plot (Fig. 13), shows that the AV remained in the region of safety during this entire period. The AV maintained a uniform velocity under the influence of the Followerstopper even if the lead demonstrated oscillatory behavior. Since the system of 21 vehicles in the ring road experiment was coupled, it resulted

in the dissipation of stop-and-go traffic waves. As a result of the same coupling, we saw that vehicle following the AV attained approximately uniform velocity, as seen in Fig. 10.

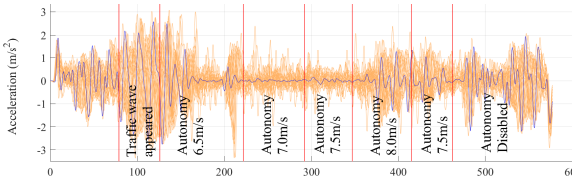

Fig. 12: Acceleration profile of all 21 vehicles involved in the final experiment to observe the wave-dampening effect of the Followerstopper.

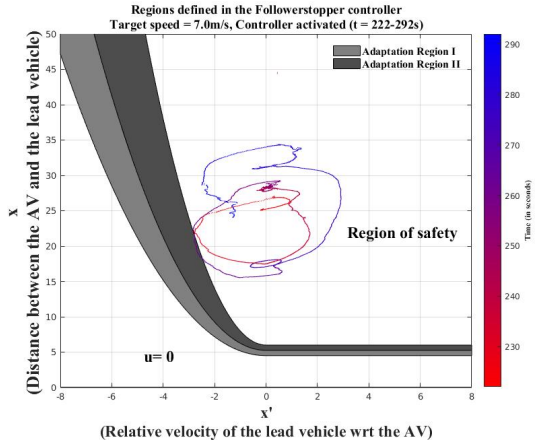

Fig. 13: Target speed set to 7.0 m/s at t=222s. In this mode of autonomy, oscillatory behavior of the AV's velocity profile is negligible. As a result of close to constant acceleration of the AV, we don't observe phase curve in the unsafe region.

At $t = 292s$, we changed reference velocity r to be $7.5m/s$ and observed the traffic behavior for next $55s$. With $r = 7.5m/s$, we observed similar kind of behavior as we saw with $r = 7.0m/s$. As described in [6] later portions of this test reflect experimentation with the velocities at which uniform flow can be achieved. Due to space limitations we leave further analysis of these portions of the experiment to future work. Remaining results of the experiment is available in [6].

VII. Conclusions and Future Work

The supervisory velocity controller presented in this paper acts as a compensator to regulate velocity control of the traffic flow, without any extensive modifications. The data obtained from the experiment validate that the controller is able to avoid collision with the vehicle ahead of it in the flow (given maximal bounds of acceleration). At the same time, the controller helps in dampening traffic waves that would otherwise cause instabilities in the flow of vehicles behind the AV. In addition, the paper demonstrates that the assumptions made on maximal bounds of acceleration and deceleration for the AV are representative of human drivers. This validates our argument that the AV's velocity controller doesn't require other vehicles in the flow to know that they are following an AV. However, in this work we don't provide any formal analysis on proving guaranteed safety of AVs using Followerstopper which is due for a future work.

VIII. Acknowledgements

This work was supported by the National Science Foundation under awards 1446715, 1446690, 1446435, and 1446702. The authors thank the University of Arizona Motor Pool for providing the vehicle fleet, Ms. Nancy Emptage for her services in carrying out the experiment logistics, and participants who made the experiment possible.

References

[1] L. Figueiredo, I. Jesus, J. T. Machado, J. R. Ferreira, and J. M. De Carvalho, "Towards the development of intelligent transportation systems," in *Intelligent Transportation Systems, 2001. Proceedings. 2001 IEEE*. IEEE, 2001, pp. 1206–1211.

[2] Y. S. Chang, Y. J. Lee, and S. S. B. Choi, "Is there more traffic congestion in larger cities?-scaling analysis of the 101 largest us urban centers," *Transport Policy*, vol. 59, pp. 54–63, 2017.

[3] Y. Sugiyama, M. Fukui, M. Kikuchi, K. Hasebe, A. Nakayama, K. Nishinari, S.-i. Tadaki, and S. Yukawa, "Traffic jams without bottlenecks - experimental evidence for the physical mechanism of the formation of a jam," *New journal of physics*, vol. 10.3, 2008.

[4] R. Jiang, C. Jin, H. Zhang, Y. Huang, J. Tian, and W. Wang, "Experimental and empirical investigations of traffic flow instability," *Transportation Research Part C: Emerging Technologies*, 2017.

[5] I.-C. Lin, C.-Y. Lin, H.-M. Hung, Q. Cui, and K.-C. Chen, "Autonomous vehicle as an intelligent transportation service in a smart city," in *86th IEEE Vehicular Technology Conference*. IEEE, 2017.

[6] R. Stern, S. Cui, M. L. D. Monache, R. Bhadani, M. Bunting, M. Churchill, N. Hamilton, R. Haulcy, H. Pohlmann, F. Wu, B. Piccoli, B. Seibold, J. Sprinkle, and D. Work, "Dissipation of stop-and-go waves via control of autonomous vehicles: Field experiments," *Transportation Research Part C: Emerging Technologies*, vol. 89, pp. 205 – 221, 2018.

[7] D. F. Llorca, V. Milanés, I. P. Alonso, M. Gavilán, I. G. Daza, J. Pérez, and M. Á. Sotelo, "Autonomous pedestrian collision avoidance using a fuzzy steering controller," *IEEE Transactions on Intelligent Transportation Systems*, vol. 12, no. 2, pp. 390–401, 2011.

[8] A. Eidehall, J. Pohl, F. Gustafsson, and J. Ekmark, "Toward autonomous collision avoidance by steering," *IEEE Transactions on Intelligent Transportation Systems*, vol. 8, no. 1, pp. 84–94, 2007.

[9] S. K. Gehrig and F. J. Stein, "Collision avoidance for vehicle-following systems," *IEEE transactions on intelligent transportation systems*, vol. 8, no. 2, pp. 233–244, 2007.

[10] M. P. Lammert, A. Duran, J. Diez, K. Burton, and A. Nicholson, "Effect of platooning on fuel consumption of class 8 vehicles over a range of speeds, following distances, and mass," *SAE International Journal of Commercial Vehicles*, vol. 7, no. 2014-01-2438, 2014.

[11] P. Kavathekar and Y. Chen, "Vehicle platooning: A brief survey and categorization," in *ASME 2011 International Design Engineering Technical Conferences and Computers and Information in Engineering Conference*. American Society of Mechanical Engineers, 2011.

[12] K.-D. Kim, "Collision free autonomous ground traffic: A model predictive control approach," in *Proceedings of the ACM/IEEE 4th International Conference on Cyber-Physical Systems*. ACM, 2013.

[13] J. E. Naranjo, C. González, R. García, and T. De Pedro, "Cooperative throttle and brake fuzzy control for acc + stop&go maneuvers," *IEEE Transactions on Vehicular Technology*, vol. 56, pp. 1623–1630, 2007.

[14] J. Naranjo, C. González, J. Reviejo, R. García, and T. De Pedro, "Adaptive fuzzy control for inter-vehicle gap keeping," *IEEE Transactions on Intelligent Transportation Systems*, vol. 4.3, pp. 132–142, 2003.

[15] M. Campbell, M. Egerstedt, J. P. How, and R. M. Murray, "Autonomous driving in urban environments: approaches, lessons and challenges," *Philosophical Transactions of the Royal Society of London A: Mathematical, Physical and Engineering Sciences*, vol. 368, no. 1928, pp. 4649–4672, 2010.

[16] R. Bhadani, M. Bunting, B. Seibold, R. Stern, S. Cui, J. Sprinkle, B. Piccoli, and D. Work, "Real-time distance estimation and filtering of vehicle headways for smoothing of traffic waves," 2019.

[17] M. Quigley, K. Conley, B. Gerkey, J. Faust, T. Foote, J. Leibs, R. Wheeler, and A. Ng, "ROS: an open-source Robot Operating System," in *ICRA workshop on open source software*, vol. 3, 2009.